applied sciences

MDPI

Article

Research on the Effects of Poly(Styrene-*co*-Butyl Acrylate) Emulsions on the Mechanical and Fracture Characteristics of Mortar

Guolin Miao [1], Peng Jiang [2], Wenxun Guan [1,3], Wanying Ma [4], Guanzhi Cheng [1,3,*], Xiangtao Li [1,3] and Yangyang Gao [2]

[1] Railway Engineering Research Institute, China Academy of Railway Sciences Co., Ltd., Beijing 100081, China; thuguanwx@163.com (W.G.)
[2] College of Materials Science and Engineering, Beijing University of Chemical Technology, Beijing 100029, China; gaoyy@mail.buct.edu.cn (Y.G.)
[3] State Key Laboratory of High-Speed Railway Track System, Beijing 100081, China
[4] School of Civil and Transportation Engineering, Beijing University of Civil Engineering and Architecture, Beijing 100044, China
* Correspondence: chengguanzhi@163.com

Abstract: A series of poly(styrene-*co*-butyl acrylate) (PSA) emulsions with different monomer ratios were synthesized and characterized, and corresponding polymer-modified mortars were prepared. The effects of polymers with different rigidities on the properties of modified mortars, including the hydration heat, mechanical strength, compressive–flexural ratio, fracture energy, and fracture toughness, were investigated. The results indicate that, as the content of hard monomers in the polymer increases, the fracture energy of the modified mortar first increases and then decreases, consistent with the changes in the polymer's damping properties. The maximum fracture energy of 211.2 N/m was achieved at a St/BA mass ratio of 4:6 and a polymer-to-cement ratio (P/C) of 15%, which was 2.4 times higher than that of the control mortar group. The fracture toughness of the modified mortar decreased with an increasing polymer doping and decreasing hard monomer content. The compressive–flexural ratio of the modified mortar decreased only with increasing the polymer emulsion dosage, showing no significant correlation with the polymer's molecular structure.

Keywords: poly(styrene-*co*-butyl acrylate) emulsions; modified mortar; mechanical characteristics; fracture characteristics

check for updates

Academic Editor: Andrei Sarbu

Received: 4 March 2025
Revised: 20 April 2025
Accepted: 22 April 2025
Published: 26 April 2025

Citation: Miao, G.; Jiang, P.; Guan, W.; Ma, W.; Cheng, G.; Li, X.; Gao, Y. Research on the Effects of Poly(Styrene-*co*-Butyl Acrylate) Emulsions on the Mechanical and Fracture Characteristics of Mortar. *Appl. Sci.* **2025**, *15*, 4822. https://doi.org/10.3390/app15094822

Copyright: © 2025 by the authors. Licensee MDPI, Basel, Switzerland. This article is an open access article distributed under the terms and conditions of the Creative Commons Attribution (CC BY) license (https://creativecommons.org/licenses/by/4.0/).

1. Introduction

Concrete is the most widely used construction material in modern civil engineering, and its performance directly impacts the safety and service life of building structures. Concrete's toughness, which measures its resistance to cracking and ability to maintain structural integrity, is particularly critical under complex conditions such as external impacts and structural deformation. This has received significant attention from researchers and engineers [1]. While concrete has an excellent compressive strength and durability compared with organic materials, its low tensile strength and toughness are major limitations, restricting its application in projects requiring high deformation and impact resistance. Building structures are evolving towards larger scales, greater complexity, and multifunctionality. To support this development trend, it has become a pressing issue to explore the mechanisms and optimization methods for enhancing concrete toughness [2]. Systematic

studies of concrete toughness can ensure the durability of traditional structures. Moreover, they can pave the way for the design and construction of new building structures.

Researchers have explored various methods to improve the toughness of concrete; for example, optimizing the concrete mix design, adjusting aggregate grading, and using special mineral admixtures can improve the microstructure of concrete, thereby enhancing its toughness. Additionally, fiber reinforcement is a common approach, with steel fibers, basalt fibers, and synthetic fibers forming a three-dimensional reinforcement system within the concrete [3–8].These fibers bridge cracks and prevent their propagation, significantly improving toughness. Polymers, as important chemical admixtures, can modify concrete by forming a continuous network structure that enhances adhesion, ductility, and durability, thereby improving crack resistance [9–13]. This enhances the deformation resistance and cracking performance of concrete. Commonly used polymers include styrene–acrylate (SA) emulsion [14], styrene–butadiene rubber (SBR) [15], and ethylene vinyl acetate (EVA) [16,17].

Polymer modification is an effective method for toughening cementitious materials. It enhances toughness, viscosity, and impermeability without significantly affecting workability; thus, it has attracted considerable research interest [18,19]. During the modification process, polymers adsorb onto the surface of hydrated cement particles and fill micropores after film formation [20], preventing crack expansion and improving toughness. However, most current studies focus on the effects of specific polymers on the toughness of cementitious materials. For example, Wang et al. [21] investigated the fracture toughness of mortar modified with butylbenzene emulsion, finding that it changed the fracture behavior from brittle to ductile. Dong et al. [22] compared the flexural strength, toughness, and impact resistance of cement concrete modified with styrene–butadiene emulsion, noting no significant correlation between these properties. Xu et al. [23] combined polypropylene fibers and SBR polymer latex to enhance mortar toughness, achieving a compressive–flexural ratio as low as 2.17 and a JCI toughness index (the ratio of the energy absorbed by the concrete specimen during the failure process to the energy absorbed when the peak load is reached [24]) of 13.1, a 258% improvement over unmodified mortar [25]. Overall, research on the relationship between polymer structure, latex film properties, and modified cementitious material toughness remains limited and requires further exploration.

In this study, five types of poly(styrene-co-butyl acrylate) (PSA) emulsions were synthesized with varying ratios of soft and hard monomers. These PSA emulsions exhibit different glass transition temperatures (T_g), minimum film-forming temperatures (MFFTs), adhesive properties, and damping characteristics. The effects of these polymer emulsions on the hydration heat, mechanical strength, compressive–flexural ratio, fracture energy, and fracture toughness of modified mortar were systematically investigated. The study focuses on elucidating the relationship between polymer composition, latex film properties, and mortar toughness, aiming to establish a preliminary framework for understanding how these factors influence the toughness of polymer-modified mortar.

2. Materials and Methods

2.1. Materials

The synthetic PSA emulsion materials are as follows: analytically pure styrene (St), butyl acrylate (BA), sodium dodecyl sulfate (SDS), and ammonium persulfate (APS), Shanghai Macklin Biochemical Technology Co., Ltd. (Shanghai, China); Emulsifier OP-10 (octylphenol polyoxyethylene), a non-ionic surfactant, Linyi Lvsen Chemical Co., Ltd. (Linyi, China); ammonia, 28–30%, Beijing Chemical Factory Co., Ltd. (Beijing, China). Deionized water was produced in the laboratory using ion exchangers. Raw materials were not purified before use.

Mortar preparation materials are as follows: reference cement, P·I 42.5 Portland cement, Fushun Cement Co., Ltd. (Fushun, China); ISO standard sand, Xiamen ISO Standard Sand Co., Ltd. (Xiamen, China); polycarboxylate superplasticizer, industrial products, Hebei Sankai Co., Ltd. (Shijiazhuang, China); P841 defoaming agent, industrial products, Munzing Chemical Group, Germany (Abstatt, Germany).

The density of the reference cement used was 3.14 g/cm^3. The test results for the chemical and mineralogical compositions of cement are shown in Table 1.

Table 1. Chemical and mineralogical compositions of cement (wt.%).

Chemical Compositions								Mineralogical Compositions			
CaO	SiO_2	Al_2O_3	Fe_2O_3	MgO	f-CaO	Na_2O	SO_3	C_3S	C_2S	C_4 AF	C_3A
65.74	22.35	4.61	3.60	2.08	0.94	0.51	0.32	56.93	21.15	11.00	6.10

2.2. Synthesis of PSA Emulsions

In this paper, PSA emulsions were synthesized using a pre-emulsified seeded semi-continuous emulsion polymerization process [26], and the typical preparation steps were as follows (as shown in Table 2):

1. Pre-emulsification: A 750 mL volume of deionized water was placed in a beaker, and 21 g of SDS and 5.25 g of OP-10 were added. The mixture was pre-dispersed for 2 min using a high-speed disperser at 10,000 rpm. The monomer mixture (750 g) was then poured into the mixture and dispersed for 10 min to obtain the monomer pre-emulsion.
2. Seed emulsion preparation: Water (100 g), SDS (2.8 g), and OP-10 (0.7 g) were placed in a three-necked flask. Then, 100 g of the monomer mixture was poured into the flask. The stirring speed was fixed at 350 rpm and the mixture was dispersed for a certain time. Once the temperature reached 80 °C, the initiator solution (0.8 g of APS dissolved in 10 mL of water) was added. The reaction proceeded for about half an hour. When the emulsion appeared light blue, the monomer pre-emulsion was added dropwise into the flask over 3 h using a peristaltic pump. The initiator solution (6 g of APS dissolved in 10 mL of water) was concurrently added into the flask dropwise over 4 h using a syringe pump. Once all the initiator solution was added, the polymerization reaction was continued at 80 °C for 1 h. Various PSA emulsions were synthesized by adjusting the pH of the reaction emulsion to 8–9 with ammonia after cooling the reaction emulsion. In this study, the mass ratios of St to BA in the mixed monomers were set to five gradients: 1:9, 2:8, 3:7, 4:6, and 5:5. The resulting emulsions were named SA1 to SA5 (in order of gradient).

Table 2. The composition and preparation process for PSA emulsions.

Step	Component	Amount	Operating Conditions
Pre-emulsification	Deionized water SDS OP-10	750 g 21 g 5.25 g	High-speed disperser, 10,000 rpm, 2 min
	Monomer mixture *	750 g	Continue dispersing for 10 min

Table 2. *Cont.*

Step	Component	Amount	Operating Conditions
Seed Emulsion Preparation	Deionized water	100 g	Stirring speed 350 rpm, heat to 80 °C
	SDS	2.8 g	
	OP-10	0.7 g	
	Monomer mixture	100 g	
	Initiator solution (APS)	0.8 g APS + 10 mL water	React for half an hour until the emulsion turns light blue
Dripping Process	Monomer pre-emulsion	750 g	Peristaltic pump, drip over 3 h
	Initiator solution (APS)	6 g APS + 10 mL water	Syringe pump, drip over 4 h
Reaction Completion	Reaction emulsion		Continue heating at 80 °C for 1 h, cool, and adjust pH with ammonia water to 8~9

* The mass ratios of St to BA in the mixed monomers of PSA emulsions were set to five gradients: 1:9, 2:8, 3:7, 4:6, and 5:5, and named SA1~SA5 (in order).

2.3. The Characterization of PSA Emulsions

The PSA emulsions were characterized using dynamic light scattering (DLS), transmission electron microscopy (TEM), a Fourier transform infrared spectrometer (FT-IR), and a differential scanning calorimeter (DSC).

The polydispersity index (PDI), (D_p^{DLS}), particle size distribution, and zeta potential of the PSA emulsions were tested using Dynamic Light Scattering (DLS) (Malvern Co., Ltd., Malvern, UK, Zetasizer Nano ZS90). For each sample, 3 repetitions were carried out to ensure result reliability. The measurements were performed at a scattering angle of 90° with the temperature maintained at 25 °C throughout. A drop of PSA emulsion was taken, dispersed in deionized water, and diluted to a concentration of about 50 ppm before being placed in the laser particle sizer for testing.

The microscopic morphologies of the PSA emulsions were tested by observing the emulsions using transmission electron microscopy (TEM) (Hitachi Co., Ltd., Tokyo, Japan, H-7650B).

The chemical structures of the PSA emulsions were tested using Fourier transform infrared spectroscopy (FT-IR) (Pike Technologies Co., Ltd., Madison, WI, USA, VERTEX 70).

The T_g of the polymer in the PSA emulsion was tested using differential scanning calorimetry (DSC) (Mettler Toledo Co., Ltd., Greifensee, Switzerland, STAR SW 16) under the following conditions: inert gas atmosphere, a heating rate of 10 °C/min, and a temperature range of 90 °C–200 °C.

The film-forming performance of PSA emulsions was tested using the minimum film formation temperature tester. The specific test process is as follows: take an appropriate amount of the emulsion, coat it uniformly on a temperature gradient plate with a circular applicator, blast air, observe the film formation of the emulsion, and determine its MFFT.

The damping properties (including the loss factor tan δ) of latex film molded with PSA emulsions were tested using a dynamic rheometer in parallel plate mode with a fixed strain of 0.1%, a frequency of 1 Hz, a heating rate of 2 °C/min, and a temperature range of −60 °C–60 °C. In addition, the latex film was treated at a high temperature before the test. On the one hand, this can completely remove the residual moisture; on the other hand, it can make the surface smoother by cooling and compressing after it becomes molten, improving the accuracy of the test.

The PSA emulsion was uniformly coated on the surface and cut surface of a 70 mm × 70 mm C40 concrete cutting block. Then, it was dried to form a film at 20 °C for 7 days. After that, an anchoring adhesive was used to bond a probe (40 mm × 40 mm) onto

the surface of the latex film. After the anchoring adhesive was cured for 24 h, an adhesion test was conducted to measure the interfacial adhesive property between the latex film and the concrete. The schematic diagram of the test is shown in Figure 1. All specimen groups were fabricated using identical proportions of the same batch of concrete. Additionally, multiple specimens were prepared per group in this experiment and tested in parallel. The discreteness of the parallel test data met the test requirements.

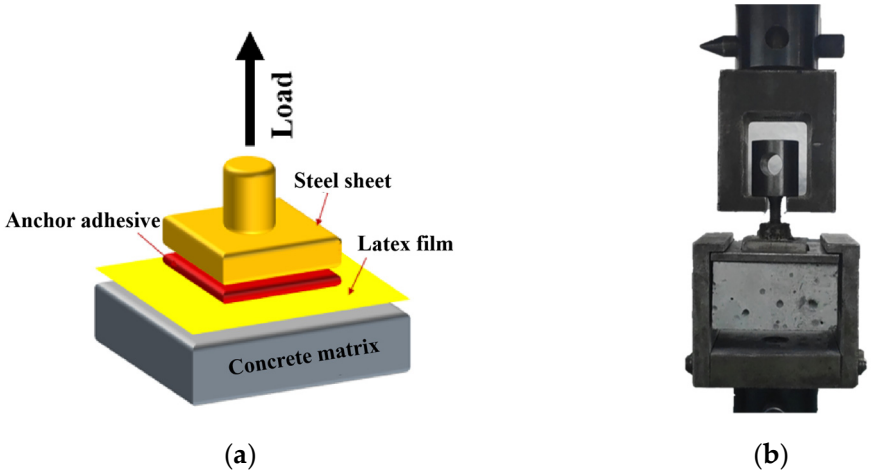


Figure 1. (**a**) A schematic diagram of the interfacial adhesion test between latex film and concrete; (**b**) the interfacial adhesion test between latex film and concrete.

2.4. The Preparation of PSA Emulsion-Modified Mortar

PSA emulsions SA1–SA5 were used to modify the mortar. A reference mortar specimen, M0, was set up without adding any PSA emulsion. The ratio parameters of the modified mortar are shown in Table 3. In addition to the reference mortar, four gradient polymer/cement (P/C) ratios were set for each type of PSA emulsion: 2.5%, 5%, 10%, and 15%. Six specimens were produced for each SA and P/C combination for each test. The P/C ratio is the mass ratio of the content of solids in the emulsion to the reference cement, and the presence of water in the emulsion should be considered when calculating water consumption.

Table 3. Mixing ratio parameters for PSA emulsion-modified mortar.

Serial Number	Reference Cement (g)	Standard Sand (g)	Water (g)	P/C Ratio (%)	Monomer Ratio in PSA Emulsion (St:BA)
M 0	675	1350	260	0	0
SA1M 2.5/5/10/15	675	1350	260	2.5/5/10/15	1:9
SA2M 2.5/5/10/15	675	1350	260	2.5/5/10/15	2:8
SA3M 2.5/5/10/15	675	1350	260	2.5/5/10/15	3:7
SA4M 2.5/5/10/15	675	1350	260	2.5/5/10/15	4:6
SA5M 2.5/5/10/15	675	1350	260	2.5/5/10/15	5:5

To ensure a good compatibility between the PSA emulsion and the mortar, the pre-wet mixing process was used to prepare the PSA emulsion-modified mortar. The typical preparation process was as follows:

The reference cement and standard sand were mixed and stirred slowly for 30 s. Then, the mixture was stirred slowly for 30 s as water was added and then for another 30 s as the PSA emulsion was poured into it. After this, the mixture was stirred slowly for 30 s, paused for 15 s, stirred slowly for 120 s, and finally stirred quickly for 60 s to obtain the

PSA emulsion-modified mortar. During the mixing process, the flow of the mortar was controlled at 205 mm ± 15 mm and the air content was controlled at 3–5% using polycarboxylate superplasticizer and P841 defoaming agent. The water in the superplasticizer and defoaming agent had been accounted for in the total water consumption.

The mixed mortar was poured into a 40 mm × 40 mm × 160 mm mold, vibrated, compacted twice on the vibrating table, and then cured. The different curing processes were as follows: (1) Standard curing for 7 days: two days of curing in a curing box (20 °C, 95% RH), demolding, and further curing for 5 days in a standard curing chamber (20 °C, 95% RH). (2) Standard curing for 28 days: two days of curing in a curing box (20 °C, 95% RH), demolding, and further curing in a standard curing room (20 °C, 95% RH) for 26 days. (3) Mixed curing for 28 days: two days of curing in the curing box, demolding, further curing in a standard curing room (20 °C, 95% RH) for 5 days, and then dry curing in a dry environment (20 °C, 60% RH) for 21 days.

2.5. The Performance Characterization of PSA Emulsion-Modified Mortar

The properties of PSA emulsion-modified mortar were characterized by testing physical properties (air content and dry density), hydration heat, and mechanical properties (flexural and compressive strength, and three-point bending test) and observing microscopic morphology.

The air content was measured directly using the air content meter (Tianjin Think Line Test Instrument Technology Co., Ltd., Tianjin, China, LS-546). The mortar was dried for 24 h at 60 °C, then for 24 h at 80 °C, and finally for 105 days. The PSA emulsion-modified mortar was cured for 28 days. It was dried at 60 °C for 24 h, then at 80 °C for 24 h, and finally at 105 °C until it reached a constant weight. After this, the density of the dry mortar was tested.

The heat of hydration of the PSA emulsion-modified mortar was tested using a microcalorimeter (TA Instruments Co., Ltd., New Castle, DE, USA, TAM-air); the instrument and test materials were kept at a constant temperature for 24 h before the test. Suitable proportions of cement, deionized water, and PSA emulsions were mixed to form a cement slurry bottle, and the water–cement ratios and polymer–cement ratios were the same as those of the modified mortar. The mixed cement slurry bottle was quickly placed into the calorimeter channel, and the heat dissipation was recorded for 7 days.

The microscopic morphology of the PSA emulsion-modified mortar was observed using a scanning electron microscope (SEM) (JEOL, Co., Ltd., Tokyo, Japan, SM-7800F). To better observe the morphology of the polymer film, the mortar was soaked in 5% hydrochloric acid for 3 h before the test. The flexural and compressive strengths of the PSA emulsion-modified mortar were tested. The specimen was 40 mm × 40 mm × 160 mm. After the flexural specimens were broken, the compressive strength test was conducted. The test process is shown in Figure 2a,b.

According to the recommendation of the RILEM technical committee [27], the fracture toughness of PSA emulsion-modified mortar was tested using a three-point bending test with a notch. Before the test, a notch with a width of 2 mm and a depth of 13.3 mm was cut out on the bottom surface of the sample with a cutting machine. Then, two 1 mm pointed iron plates were used to fix the clamp extender on both sides of the notch to measure the crack mouth opening displacement (CMOD), and the loading speed was set to 0.5 mm/min. The test process is shown in Figure 2c.

The fracture energy (G_f) of notched mortar strips was calculated using Equation (1) when performing the three-point bending test, as follows

$$G_f = \frac{W_0 - mg\partial_0}{A_{lig}} \quad (1)$$

where W_0 is the area of the load–deflection curve, mg is the self-weight of the mortar strip, ∂_0 is its deflection corresponding to the maximum load, and A_{lig} is the area of the fracture surface $[B(W - a_0)]$, where B is the width of the mortar strip, W is the height of the mortar strip, and a_0 is the initial crack length.



(**a**) (**b**) (**c**)

Figure 2. (**a**) Flexural strength tests of PSA emulsion-modified mortar. (**b**) Compressive strength tests of PSA emulsion-modified mortar. (**c**) The fracture toughness test setup for PSA emulsion-modified mortar.

The two-parameter method [28] was used to calculate the fracture toughness of the modified mortar, as shown in Equation (2). This method can directly calculate the critical stress intensity factor; that is, the fracture toughness (K_{IC}), which can be used to measure the crack propagation resistance of the material, as follows:

$$K_{IC} = \frac{3P_{max}S}{2W^2B}\sqrt{\pi \underline{a}}F(\alpha) \tag{2}$$

where P_{max} is the maximum load, S is the distance between the two support points at the bottom of the specimen, $\underline{a}$ is the effective crack length, and $F(\alpha)$ is calculated as in Equation (3):

$$F(\alpha) = \frac{1}{\sqrt{\pi}}\frac{1.99 - \alpha(1-\alpha)\left(2.15 - 3.95\alpha + 2.7\alpha^2\right)}{(1+2\alpha)(1-\alpha)^{\frac{3}{2}}} \tag{3}$$

where α is a_0/W.

The modulus of elasticity E of the modified mortar is measured from the initial flexibility C_i as in Equation (4):

$$E = \frac{6Sa_0V_1(\alpha)}{C_iW^2B} \tag{4}$$

where a_0 is the initial notch depth, and $V_1(\alpha)$ is calculated as in Equation (5):

$$V_1(\alpha) = 0.76 - 2.28\alpha + 3.78\alpha^2 - 2.04\alpha^3 + \frac{0.66}{(1-\alpha)^2} \tag{5}$$

where $\alpha = \frac{(a_0+H_0)}{(W_0+H_0)}$, which takes into account the effect of the thickness of the clip-on extensometer gasket H_0.

3. Results and Discussion

3.1. The Effects of Different Monomer Ratios on the Performance of the Various Synthesized PSA Emulsions

Of the two monomers in the PSA emulsion, St is a hard monomer due to its benzene ring structure, while butyl acrylate is a soft monomer due to its linear structure. The use of different ratios of soft and hard monomers leads to significant changes in the rigidity of

the polymer chain segment in the emulsion and significant changes in its performance [29]. Thus, a series of PSA emulsions with different monomer ratios were initially characterized with the aim of investigating the effects of the soft and hard monomer ratios on the performance of PSA emulsions.

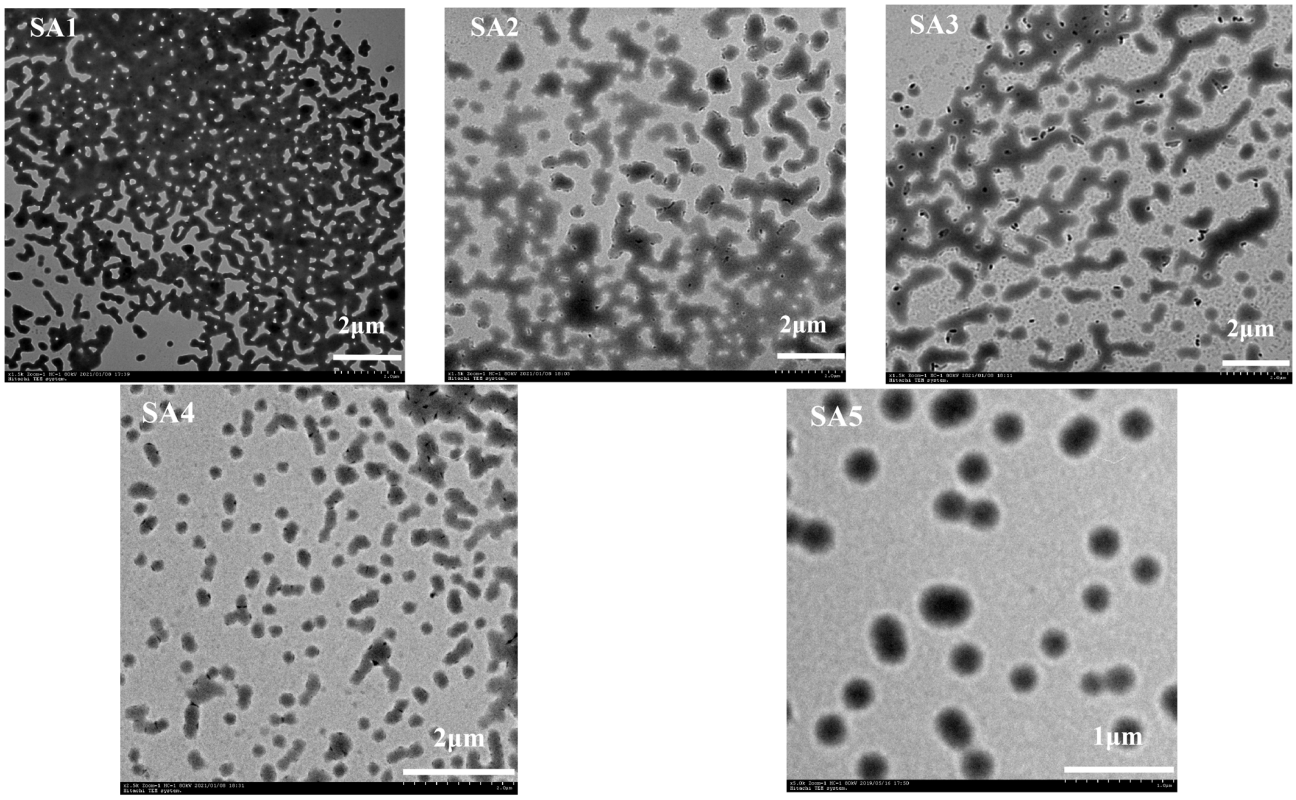
Firstly, the basic performance of the various synthesized PSA emulsions was tested; the results are shown in Table 4. The PDI is used to describe the uniformity of the molecular weight distribution in the polymer; the smaller the PDI value, the more uniform the molecular weight distribution. It shows that the series of PSA emulsions synthesized using pre-emulsified semicontinuous seeded emulsion polymerization have a high conversion ($\geq$95%) and low PDI (<0.08), which indicates that this polymerization method is more suitable for the polymerization of the present system and the emulsion particles are well dispersed during polymerization. The hydrodynamic diameter is the particle size of the composite particles in the emulsion state. The hydrodynamic diameter of the emulsion is approximately 160 nm. The zeta potential refers to the potential difference between the surface of polymer particles and the surrounding fluid, which is an important indicator for characterizing the stability of the polymer dispersion system; the higher the absolute value of the zeta potential, the better the stability. The zeta potentials are all negative values, indicating that the surface is negatively charged, and the absolute value of the zeta potential is more than 50 mV, which indicates that the anionic emulsifier and nonionic emulsifier compounding system used in this paper can effectively stabilize the PSA emulsion [30].

Table 4. Basic properties of PSA emulsions.

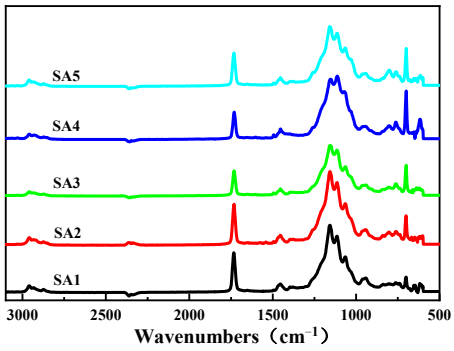
Serial Number	Monomer Ratio (St:BA)	PDI	D_p^{DLS} (nm)	Zeta Potential (mV)	Solid (%)	Conversion Rate (%)	T_g (°C)	MFFT (°C)
SA1	1:9	0.063	160.9	−61.0	48.8	95	−42.4	<−5
SA2	2:8	0.050	153.8	−52.5	50.0	98	−26.6	<−5
SA3	3:7	0.032	160.3	−50.1	49.8	98	−11.9	<−5
SA4	4:6	0.047	159.4	−54.3	49.3	96	1.5	−0.4
SA5	5:5	0.063	151.4	−51.2	48.9	95	18.91	12.6

The test results of the glass transition temperature (T_g) and the minimum film-forming temperature (MFFT) show that, as the content of the hard monomer (St) gradually increases in the mixed monomers, the T_g and MFFT also gradually increase. This is mainly because the increase in the content of the hard monomer enhances the rigidity of the polymer chain segments and reduces the free movement of these segments, hence the T_g gradually increases. One of the most important steps in the film forming process of the polymer latex is the mutual fusion between the latex particles. Therefore, the movement of the chain segments is extremely crucial. This also leads to a strong correlation between the MFFT and T_g in general; thus, the MFFT also gradually increases with an increase in the St content. However, the MFFTs of the PSA emulsions in this paper are significantly lower than the conventional curing temperature of mortar, which is 20 °C. This ensures that the PSA emulsions have good film forming properties in mortar.

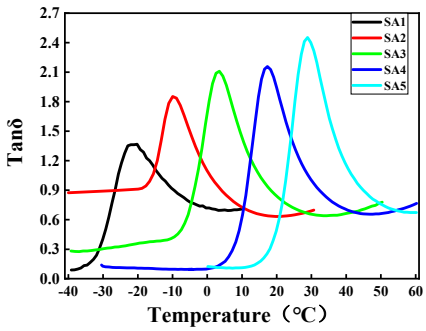
The TEM results of the microstructure of PSA emulsions are shown in Figure 3a. The latex particles show a more uniform spherical structure, with sizes similar to the DLS test results. The latex particles can be easily bonded together to form a film under a low St content, while the granular structure of the latex particles becomes more obvious as the St content gradually increases. This is mainly because the PSA emulsion with the low St content easily forms a film during the TEM sampling process.



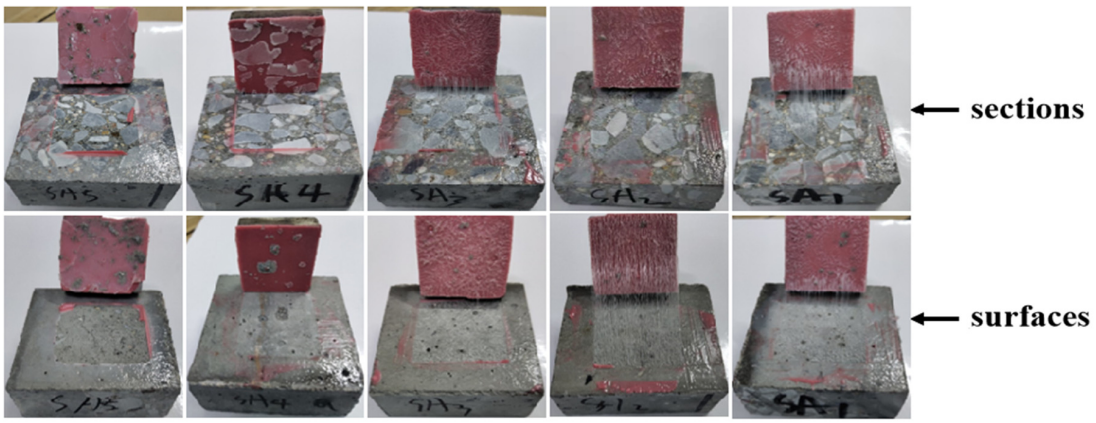
(**a**)



(**b**)



(**c**)



(**d**)

Figure 3. (**a**) TEM images of various PSA emulsions. (**b**) FT-IR test results of the various PSA emulsions. (**c**) Damping properties of PSA latex film. (**d**) The fracture surface of an adhesion test specimen.

The chemical structures of the synthesized PSA emulsions were tested using FT-IR; the test results are shown in Figure 3b. All the prepared PSA emulsion latex films exhibit C=O stretching vibration peaks in the ester group at 1710 cm^{-1}–1740 cm^{-1}, and C-O stretching vibration peaks in the 1050 cm^{-1}–1300 cm^{-1} region, which confirms the presence of ester groups in the polymer. The characteristic absorption peaks of monosubstituted benzene rings distributed at 690 cm^{-1}–700 cm^{-1} and 740 cm^{-1}–750 cm^{-1} are also found in the PSA series latex films, which effectively indicates the presence of a benzene ring structure in the polymer latexes. In addition, the characteristic peaks at 740 cm^{-1}–750 cm^{-1} are elevated from SA1 to SA5. This is also consistent with the presence of ester groups in the polymer. The above results prove that the molecular structures of the PSA emulsion films are the same as those of the designed structure.

The damping performance results of the PSA latex films are presented in Figure 3c. As the St content increases, the damping temperature range of the latex film gradually increases and the peak value of the loss factor also gradually increases. This phenomenon is chiefly attributed to the fact that, compared with BA, St features a larger rigid steric hindrance group. On one hand, this leads to a weaker mobility of the polymer chain segments and the temperature range within which damping occurs is expanded; on the other hand, energy dissipation becomes more pronounced during the movement of these chain segments, causing the peak value of the loss factor to increase continuously. Moreover, given that the service and performance-related tests on mortar are conducted at ambient temperature, the damping performance of the PSA latex films at this temperature is ranked as follows: SA4 > SA5 > SA3 > SA2 > SA1.

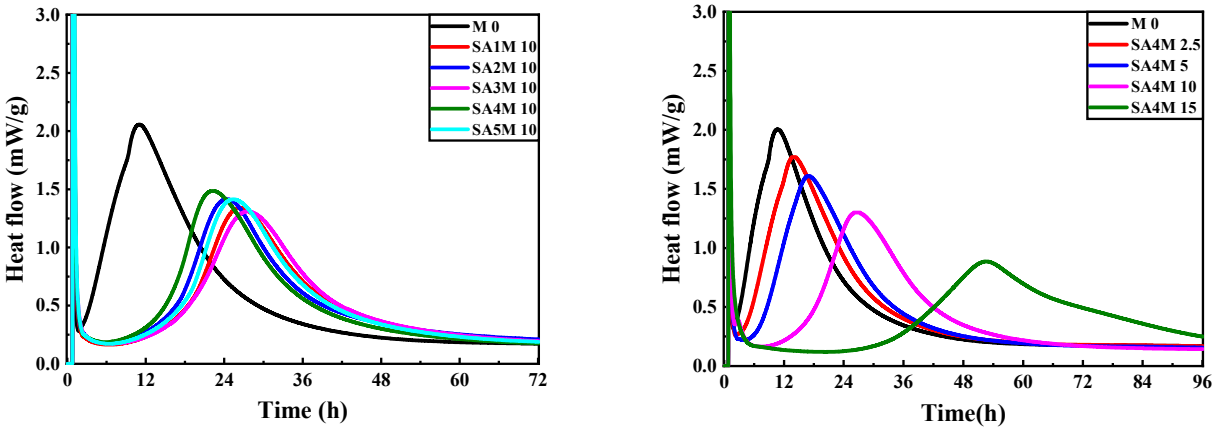
The adhesive property of PSA emulsions with concrete were tested using the positive tensile adhesion test. The results are shown in Figure 3d and Table 5. It can be seen that as the content of St increases, the adhesion strength shows a generally increasing trend. This is because at room temperature, the latex film with a lower St content has a relatively low strength, making it prone to cohesive failure within the latex film layer. As the St content increases, the strength of the latex film gradually improves. The microscopic interlocking effect that contributes to adhesion also increases accordingly, and the adhesion strength gradually rises. This can also be inferred from the adhesion failure modes of the latex films. For SA1, SA2, and SA3, the failure mode is the rupture of the latex film itself. For SA4, adhesion failure occurs at the interface between the latex film and the concrete. For SA5, adhesion failure is a combination of the failure at the adhesion interface and the failure of the concrete matrix. The adhesion strength is significantly improved at room temperature.

Table 5. Adhesion test results for different concrete surfaces.

Serial Number	Latex Film Formation on Concrete Sections		Latex Film Formation on Concrete Surfaces	
	Adhesion Strength (MPa)	Forms of Damage	Adhesion Strength (MPa)	Forms of Damage
SA1	0.57	Latex film body damage	0.34	Latex film body damage
SA2	0.42	Latex film body damage	0.22	Latex film body damage
SA3	0.57	Latex film body damage	0.31	Latex film body damage
SA4	1.64	Interfacial damage between latex film and concrete	1.21	Interfacial damage between latex film and concrete
SA5	3.53	Interfacial damage/concrete matrix damage	3.41	Interfacial damage/concrete matrix damage

3.2. Effects of PSA Emulsions on the Heat of the Hydration of Modified Mortar

Since the added PSA emulsion is wrapped on the surface of cement particles, it usually hinders the hydration of cement mortar. Here, we tested the effects of adding different ratios and different dosages of PSA emulsion on the exothermic course of the hydration of cement mortar. The specific results are shown in Figure 4.



(**a**) (**b**)

Figure 4. The hydration heat release rate of PSA emulsion-modified paste: (**a**) different emulsions with the same dosage; (**b**) SA4 emulsion with different dosages.

Figure 4a shows that all PSA emulsions can delay cement hydration. While reducing the peak value of the hydration heat release rate, they also postpone the time at which the peak value occurs; however, the differences between different PSA emulsions are very small. This may be because the types and ratios of emulsifiers used in the PSA emulsions are the same, resulting in very small differences in the zeta potentials of PSA emulsions. The differences in the adsorption properties of these emulsions on cement are not significant, which in turn leads to very small differences in the effects of different PSA emulsions on the hydration heat release rate.

Figure 4b shows the hydration heat test results of the neat pastes modified with SA4 emulsion at different dosages. As the P/C ratio increases, the peak value of the hydration heat release rate continuously decreases, and the time when the peak value occurs is continuously postponed. When the P/C ratio is 15%, the time when the peak value of the heat release rate occurs exceeds 48 h, which is approximately four times that of the blank mortar. The peak value of the heat release decreases significantly, being less than half that of the blank mortar. When the dosage of the emulsion is relatively high, its inhibitory effect on the hydration of cement is more obvious, which is bound to impact the early mechanical properties and toughness of the series of PSA emulsion-modified mortars.

3.3. The Effects of PSA Emulsions on the Mechanical Properties of Modified Mortar

The mechanical properties of the polymer-modified mortar were characterized based on compressive strength, flexural strength, and the compressive–flexural ratio. The test results in Figure 5 show that for all the PSA emulsions, the compressive strengths of the modified mortars continuously decrease with increasing P/C ratios at different ages and curing methods. When the P/C ratio is 15%, the compressive strength of the modified mortars is nearly 50% lower than that of the blank mortar. Furthermore, there is also a correlation between the compressive strength of the modified mortars and the composition of the PSA emulsions: the compressive strength of the modified mortars is relatively higher for the PSA emulsions with a higher content of the hard monomer St. Comparing the

compressive strengths of the modified mortars at different ages shows that the compressive strength of the blank mortar M0 increases from less than 50 MPa at the curing age of 7 days to about 72 MPa at the curing age of 28 days. For the five types of mortars modified with PSA emulsions, the growth rate of the compressive strength decreases significantly with the increase in the P/C ratio as the curing age increases. In particular, when the P/C ratio is 15%, the increase is less than 10 MPa. This may be due to the following two reasons: (1) The incorporated PSA emulsion replaces part of the cementitious material, and the more emulsion is added, the larger the proportion of the replaced cementitious materials. This leads to a smaller increase in the later strength of the modified mortar. (2) The PSA emulsion hydrolyzes under the alkaline conditions after cement hydration [31], forming carboxyl groups that combine with Ca^{2+}, thus reducing the generation of other hydration products. Moreover, more hydrolyzed groups are produced and the amount of other hydration products decreases as the dosage of the PSA emulsion increases, resulting in an unobvious increase in the compressive strength.

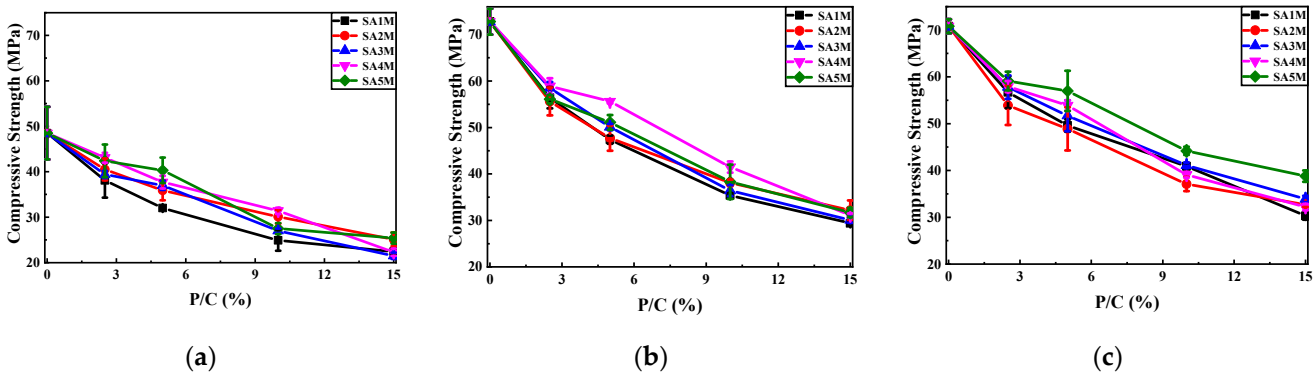


Figure 5. Compressive strengths of a series of PSA emulsion-modified mortars: (**a**) 7 days standard curing; (**b**) 28 days standard curing; (**c**) 28 days mixed curing.

The five PSA emulsions had different effects on the compressive strength of the mortar under different curing conditions. Under mixed curing conditions, the compressive strength of SA5M was approximately 7 MPa higher than under standard curing; in contrast, there was no significant change in the compressive strengths of the modified mortars of the other four PSA emulsions. This is mainly due to the fact that SA5 emulsion has the highest minimum film-forming temperature, which is slightly lower than the mortar curing temperature and is easily affected by the curing method. Mixed curing includes dry curing, which is conducive to the film formation of polymer emulsion. This, in turn, influences the properties of the latex film after it has formed. As a result, different curing methods significantly impact the compressive strength of the modified mortar. However, the minimum film-forming temperatures of the other four types of PSA emulsions are much lower than the curing temperature. Consequently, the influence of different curing methods on their film-forming properties is limited, and thus the impact on their compressive strength is also limited.

The curves of the variations in flexural strength with P/C of the modified mortars with PSA emulsions are shown in Figure 6. For the five types of PSA emulsions, the flexural strengths of the modified mortars produced for different periods under different curing conditions decrease with increasing P/C ratios. This may be because the content of BA in the PSA emulsion is too high, resulting in excessive chemical reactions during cement hydration and leading to a decrease in strength. There is no obvious relationship between the flexural strength of the mortars modified with different PSA emulsions and the composition of the PSA emulsions. However, the flexural strength of 28-day-old SA5M

is generally higher than those of the other four types of modified mortars under different P/C ratios.

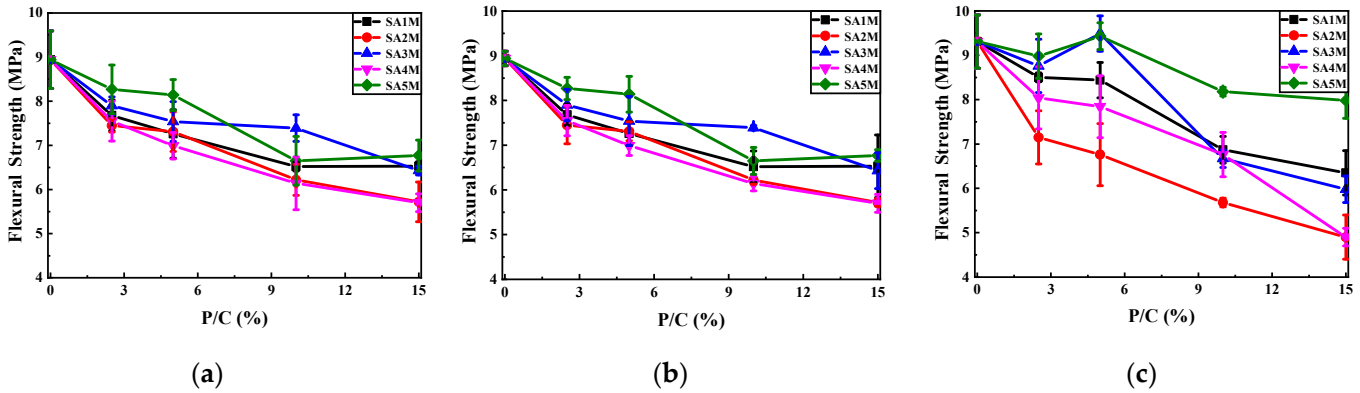


Figure 6. The flexural strength of a series of PSA emulsion-modified mortars: (**a**) 7 days standard curing; (**b**) 28 days standard curing; (**c**) 28 days mixed curing.

Comparing the flexural strengths of the mortars modified with the series of PSA emulsions for different periods shows that the flexural strength does not increase significantly as the curing age increases. In particular, the increase is limited when the P/C ratio is 15%. Comparing the influence of different curing methods on the flexural strengths of the mortars modified with the five types of PSA emulsions shows that at a low P/C ratio, the flexural strength of the modified mortar under mixed curing is higher than under standard curing. This is associated with the fact that dry curing in the mixed curing method is beneficial to film formation. However, when the high P/C ratio is 15%, the opposite result is true, especially for SA1M and SA2M.

The compressive–flexural ratios for the mortars modified with the series of PSA emulsions are obtained from the compressive and flexural strength test results. The results are shown in Figure 7. For different curing periods and methods for the five types of PSA emulsions, the compressive–flexural ratios of the modified mortars generally show a trend of gradually decreasing with increasing P/C ratios. The lowest value is 3.44, indicating that the toughness of the modified mortar is improving. However, there is no obvious relationship between the compressive–flexural ratios of the mortars modified with different PSA emulsions, the compositions of the five types of PSA emulsions, and the properties of the latex films, and the variations are irregular. In addition, the compressive–flexural ratios of SA2M and SA4M are significantly higher than those of the three other types of modified mortars, while the toughening effects are worse. The compressive–flexural ratio of the modified mortar increases the curing age, while the toughness reduces. Different curing methods have little effect on the compressive–flexural ratio of the mortars modified with the series of PSA emulsions.

Figure 8 shows that adding PSA emulsion to the mortar reduces the modulus of elasticity of the mortar, making it flexible. The modulus of elasticity of the mortar gradually decreases with increasing P/C ratios, with the lowest value being approximately half that of the blank mortar. The elastic modulus of the modified mortar increases with curing age. There are minor differences in the elastic modulus values of the five types of mortars modified with PSA emulsions at each P/C ratio. The influence of different curing methods on the elastic modulus is also limited.

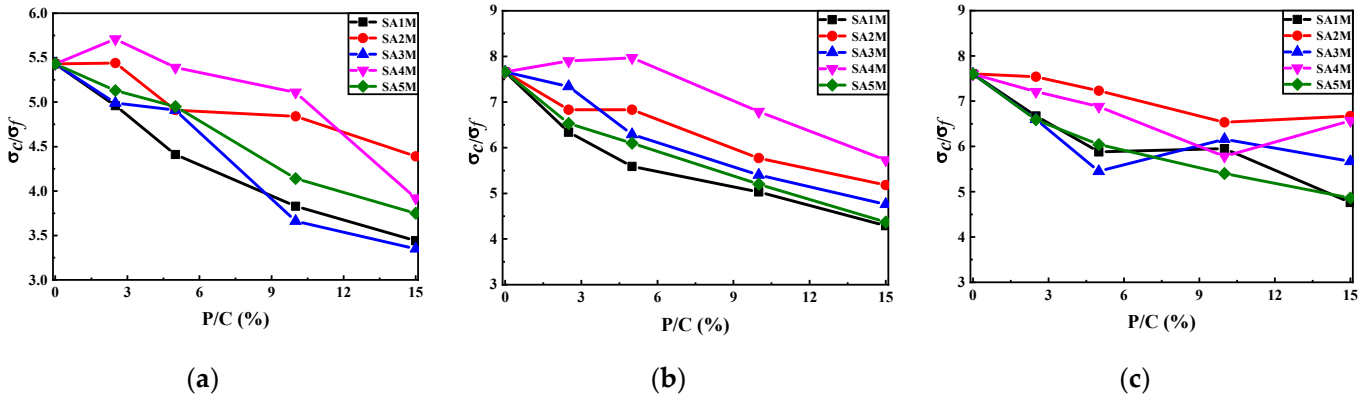


Figure 7. Compressive–flexural ratios for a series of PSA emulsion-modified mortars: (**a**) 7 days standard curing; (**b**) 28 days standard curing; (**c**) 28 days mixed curing.

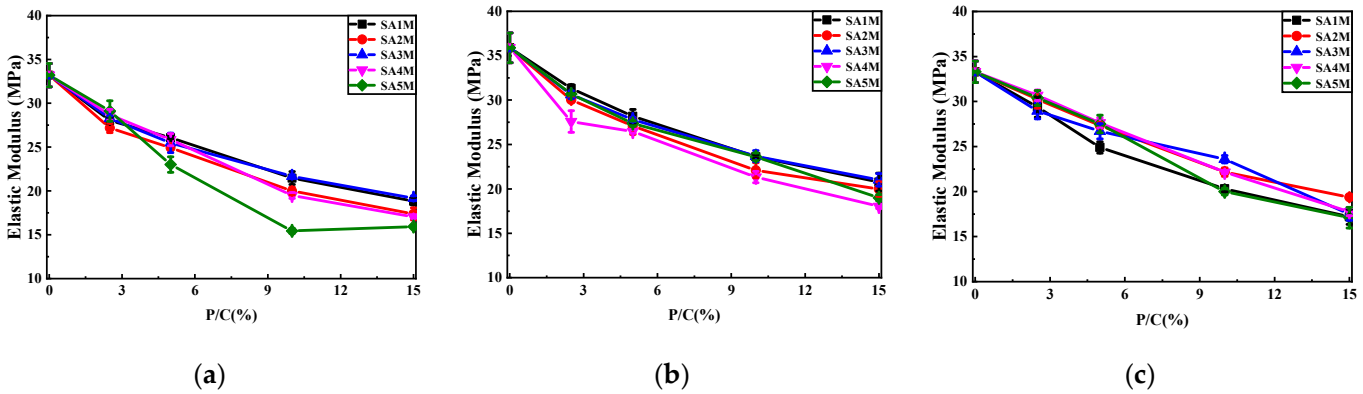


Figure 8. The variation in the modulus of elasticity with P/C ratios for PSA emulsion-modified mortars: (**a**) 7 days standard curing; (**b**) 28 days standard curing; (**c**) 28 days mixed curing.

3.4. The Effects of PSA Emulsions on the Fracture Properties of Modified Mortar

The fracture energies of the mortars modified with the series of PSA emulsions can be obtained by testing the load and mid-span deflection curves of the polymer-modified mortars. The results are shown in Figure 9. The fracture energies of both SA1M and SA2M are lower than that of the blank mortar for different curing ages and methods, and the fracture energy reduces with increasing P/C ratios. This is mainly because the content of the soft monomer BA in the SA1 and SA2 emulsions is too high, resulting in a significant influence of the chemical reactions of the PSA emulsions in the cement-based materials. While forming a nested membrane structure, it has an obvious impact on other hydration products, which not only reduces the mechanical properties of the mortar but also decreases its toughness. In addition, it is worth noting that the test results of the compressive–flexural ratios show that the compressive–flexural ratio of SA1M is lower than that of the other types of modified mortars, and thus its toughness should be better. This may be because the five types of PSA emulsions reduce the compressive and flexural strengths, making the compressive–flexural ratio unsuitable for this system.

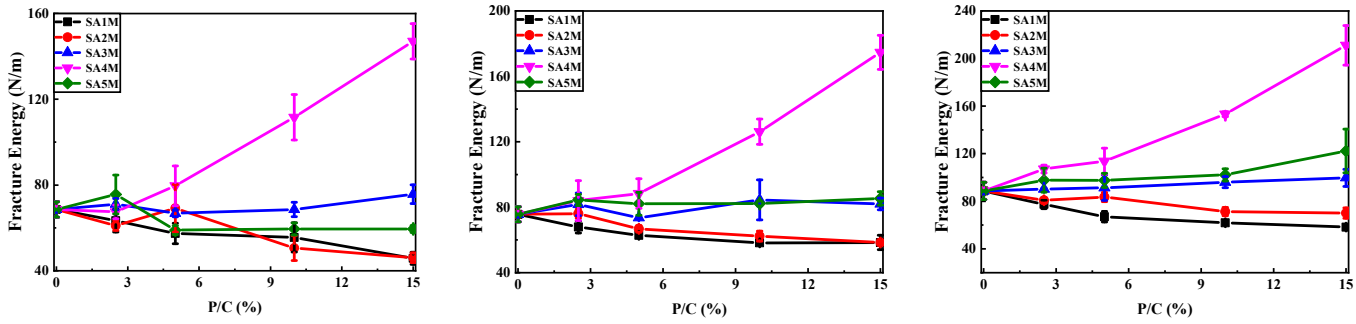


Figure 9. The variation in fracture energy as a function of P/C for five PSA emulsion-modified mortars: (**a**) 7 days standard curing; (**b**) 28 days standard curing; (**c**) 28 days mixed curing.

The fracture energy of SA3M is slightly higher than that of the blank mortar at different curing ages and with different methods. The differences in fracture energies between the modified mortars are very small at different P/C ratios. The fracture energy value for SA4M increases with an increasing P/C ratio. When the P/C ratio is 15%, its maximum fracture energy is 211.2 N/m, approximately 2.4 times that of the blank mortar. This is the highest fracture energy among the mortars modified with the five types of PSA emulsions. The results of the compressive–flexural ratio show that the compressive–flexural ratio of SA4M is higher and the toughness is lower compared with the other five types of modified mortars, which further confirms that it is not suitable for this system. In addition, its maximum fracture energy at 7 days of curing is 2.1 times that of the blank mortar, indicating that the SA4 emulsion has formed a film and plays a role even when the hydration is incomplete. At 7 days of curing, the change in fracture energy with the P/C ratio for SA5M is similar to that of SA1M and SA2M, and the fracture energy is significantly lower than that of the blank mortar. The fracture energy of SA5M is slightly higher than that of the blank mortar at 28 days under the standard curing condition. The fracture energy of SA5M increases with the increase in the P/C ratio at 28 days of curing under the mixed curing condition, and the range of the increase is much higher than that under the standard curing condition at 28 days of curing. The highest value is approximately 1.4 times that of the blank mortar. The fracture energy of SA5M is the most affected by the curing method. This is mainly because the content of the hard monomer St in the SA5 emulsion is high, and its T_g and MFFT are highest, only slightly lower than the cement curing temperature. The polymer does not form a film under the wet curing condition of standard curing, resulting in a lower fracture energy; however, the polymer forms a film under the mixed curing condition with dry curing, which significantly increases its fracture energy. The influence of the series of PSA emulsions on the fracture energy of the mortar follows a similar pattern at different ages and with different curing methods: SA1 < SA2 < SA3 < SA5 < SA4. The optimal composition ratio of St to BA in the PSA emulsion is 4:6. Increasing St content and decreasing BA content in the PSA emulsion first increases and then decreases the fracture energy of the modified mortar. In Figure 10a, each curve represents mortars with the same P/C ratio. As the damping performance of the PSA emulsion latex film increases, the fracture energy of the modified mortar first decreases and then increases. However, the adhesion performance shows a correlation different from the damping performance, and an effective relationship cannot be established here (Figure 10b).

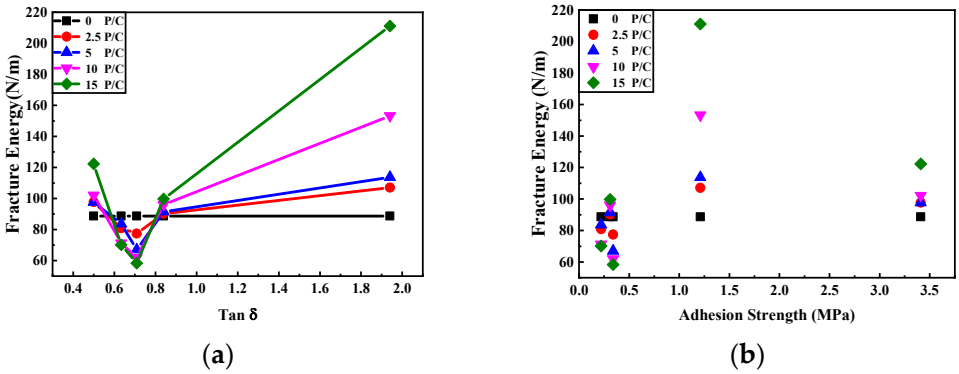


Figure 10. (**a**) The variation in fracture toughness as a function of the damping property of the latex film. (**b**) The variation in fracture toughness as a function of the adhesive properties of the latex film.

As shown in Figure 11, the results of the fracture toughness are different from those of the fracture energy. The fracture toughness of the mortars modified with the series of PSA emulsions is lower than that of the blank mortar at different ages, under different curing conditions, and at different dosages. The fracture toughness of the modified mortars generally shows a gradually decreasing trend with increasing P/C ratios, with the lowest value being approximately 0.4 MPa·m$^{1/2}$, which is nearly half that of the blank control group. This may be because the addition of the emulsion leads to a reduction in cementitious materials, and the chemical reaction between them significantly affects the generation of hydration products, resulting in a significant decrease in the maximum load of the modified mortar. Comparing fracture toughness differences between different PSA emulsion-modified mortars shows that the differences are not significant at 7 days of curing. There is no obvious correlation with the composition of the PSA emulsion itself and the performance of the latex film. However, at 28 days, the fracture toughness values seem to show a linear arrangement, with the following order: SA5M > SA4M > SA3M > SA2M > SA1M.

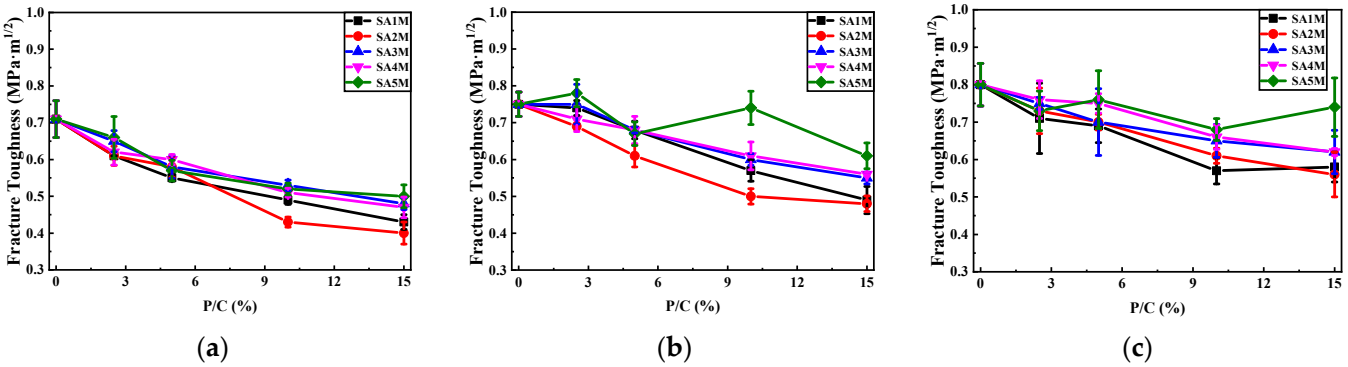


Figure 11. The variation in fracture toughness as a function of the P/C ratio for mortars modified with different PSA emulsions: (**a**) 7 days standard curing; (**b**) 28 days standard curing; (**c**) 28 days mixed curing.

The fracture toughness of the modified mortar increases to a certain extent with the increase in age, and there is little difference in the range of increase of the mortars modified with different emulsions. In addition, the fracture toughness of the modified mortar under mixed curing was higher than under standard curing, indicating that dry curing is favorable for polymerization film formation, thus improving the toughness of its modified mortar.

3.5. The Microscopic Morphology of PSA Emulsion-Modified Mortar

The micro-morphologies of the reference mortar and the polymer-modified mortar were compared using SEM, and the results are shown in Figure 12. The figure shows that

after acid treatment, SA4M 15 had a higher structural density than M0. The addition of SA4 emulsion significantly improved the chemical corrosion resistance of the mortar. SA4M 15 had a large number of polymer films that formed an inter-nested structure with the mortar. The presence of the large number of polymer films and the excellent damping performance of the latex film are the reasons for the high fracture energy of SA4M 15.

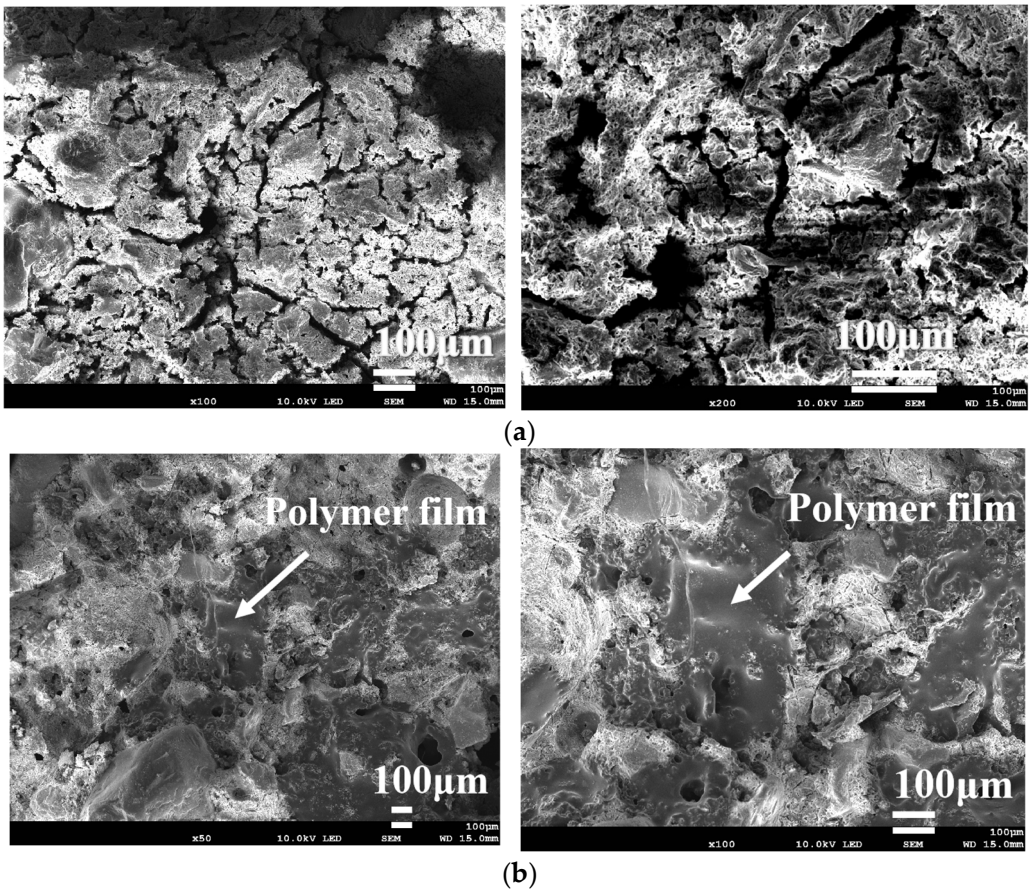


Figure 12. The microscopic morphology of mortar: (**a**) M 0; (**b**) SA4M 15.

4. Conclusions

This paper systematically investigates the relationship between the composition of a series of PSA emulsions, the performance parameters of the latex film, the compression-fold ratio, the fracture energy, and the fracture toughness of their modified mortars. The conclusions drawn are as follows:

1. With an increase in the relative content of St in the PSA emulsion, the fracture energy of the formulated modified mortar first increases and then decreases, consistent with the pattern of change in the damping properties of the latex film. Among them, the fracture energy of modified mortar SA4M 15 is the highest, reaching 211.2 N/m, which is approximately 2.4 times that of the blank mortar control group.
2. The compressive–flexural ratios of the series of PSA emulsion-modified mortars are associated with the polymer emulsion dosage; they decrease as the P/C ratio increases, with a minimum value of 3.44. However, there is no obvious correlation between the compressive–flexural ratio and the composition of the PSA emulsions themselves, as well as the performance parameters of the latex films.
3. The fracture toughness of the series of PSA emulsion-modified mortars is also associated with polymer emulsion doping. The maximum load of the fracture test decreases significantly with an increase in P/C ratio, and the fracture toughness also decreases.

The lowest value is approximately 0.4 MPa·m$^{1/2}$, which is nearly half that of the control group. At the same dosage, the fracture toughness increases with an increase in the proportion of St monomer in the PSA emulsion, although there is no obvious relationship with the damping performance parameters of the latex film.

Author Contributions: G.M.: Writing—original draft, investigation, resources; P.J.: writing—original draft and investigation; W.G.: writing—review and editing, and validation; W.M.: writing—review and editing, and methodology; G.C.: writing—review and editing, and funding acquisition; X.L.: validation and resources; Y.G.: writing—review and editing, and funding acquisition. All authors have read and agreed to the published version of the manuscript.

Funding: This work was supported by the National Natural Science Foundation of China (No. 52478290) and by the Fund of China Academy of Railway Sciences (2022YJ129).

Institutional Review Board Statement: Not applicable.

Informed Consent Statement: Not applicable.

Data Availability Statement: Data will be made available on request.

Acknowledgments: We extend our sincere gratitude to Yongjiang Xie and Yanbin Tan for their invaluable technical guidance.

Conflicts of Interest: Authors W.G., G.C. and X.L. were employed by the company Railway Engineering Research Institute, China Academy of Railway Sciences Co., Ltd. The remaining authors declare that the research was conducted in the absence of any commercial or financial relationships that could be construed as a potential conflict of interest.

References

1. Ding, Y.; Guo, W.; Li, D.; Pacheco-Torgal, F. Exploring the Effect of Polyoxymethylene Fiber on Concrete Toughness and Self-Sensing Capability of Concrete Cracking under Bending. *Constr. Build. Mater.* **2024**, *454*, 138933. [CrossRef]
2. Tian, C.; Zheng, Z.; Wei, X. A New Fracture Toughness Calculation Method for Cementitious Materials in the Three-Point Bending Test Based on the Transverse Force. *Case Stud. Constr. Mater.* **2022**, *17*, e01215. [CrossRef]
3. Guo, H.; Jiang, L.; Tao, J.; Chen, Y.; Zheng, Z.; Jia, B. Influence of a Hybrid Combination of Steel and Polypropylene Fibers on Concrete Toughness. *Constr. Build. Mater.* **2021**, *275*, 122132. [CrossRef]
4. Li, J.J.; Wan, C.J.; Niu, J.G.; Wu, L.F.; Wu, Y.C. Investigation on Flexural Toughness Evaluation Method of Steel Fiber Reinforced Lightweight Aggregate Concrete. *Constr. Build. Mater.* **2017**, *131*, 449–458. [CrossRef]
5. Yan, S.; Dong, Q.; Chen, X.; Li, J.; Wang, X.; Shi, B. An Experimental and Numerical Study on the Hybrid Effect of Basalt Fiber and Polypropylene Fiber on the Impact Toughness of Fiber Reinforced Concrete. *Constr. Build. Mater.* **2024**, *411*, 134270. [CrossRef]
6. Ding, Y.; Wang, Q.; Pacheco-Torgal, F.; Zhang, Y. Hybrid Effect of Basalt Fiber Textile and Macro Polypropylene Fiber on Flexural Load-Bearing Capacity and Toughness of Two-Way Concrete Slabs. *Constr. Build. Mater.* **2020**, *261*, 119881. [CrossRef]
7. Alimrani, N.S.; Balazs, G.L. Toughness and Stiffness of Fibre Reinforced Concrete in Terms of Shear Capacity. *Constr. Build. Mater.* **2023**, *389*, 131711. [CrossRef]
8. Richardson, A.; Coventry, K.; Lamb, T.; Mackenzie, D. The Addition of Synthetic Fibres to Concrete to Improve Impact/Ballistic Toughness. *Constr. Build. Mater.* **2016**, *121*, 612–621. [CrossRef]
9. Ohama, Y. Polymer-Based Admixtures. *Cem. Concr. Compos.* **1998**, *20*, 189–212. [CrossRef]
10. Chama, Y. Principle of Latex Modification and Some Typical Properties of Latex-Modified Mortars and Concretes. *ACI Mater* **1987**, *84*, 511–518.
11. Sakai, E.; Sugita, J. Composite Mechanism of Polymer Modified Cement. *Cem. Concr. Res.* **1995**, *25*, 127–135. [CrossRef]
12. Rashid, K.; Ahmad, M.; Ueda, T.; Deng, J.; Aslam, K.; Nazir, I.; Azam Sarwar, M. Experimental Investigation of the Bond Strength between New to Old Concrete Using Different Adhesive Layers. *Constr. Build. Mater.* **2020**, *249*, 118798. [CrossRef]
13. Moodi, F.; Kashi, A.; Ramezanianpour, A.A.; Pourebrahimi, M. Investigation on Mechanical and Durability Properties of Polymer and Latex-Modified Concretes. *Constr. Build. Mater.* **2018**, *191*, 145–154. [CrossRef]
14. Zhang, X.; Li, G.; Song, Z. Influence of Styrene-Acrylic Copolymer Latex on the Mechanical Properties and Microstructure of Portland Cement/Calcium Aluminate Cement/Gypsum Cementitious Mortar. *Constr. Build. Mater.* **2019**, *227*, 116666. [CrossRef]
15. Yang, Z.; Shi, X.; Creighton, A.T.; Peterson, M.M. Effect of Styrene–Butadiene Rubber Latex on the Chloride Permeability and Microstructure of Portland Cement Mortar. *Constr. Build. Mater.* **2009**, *23*, 2283–2290. [CrossRef]

16. Betioli, A.M.; Gleize, P.J.P.; John, V.M.; Pileggi, R.G. Effect of EVA on the Fresh Properties of Cement Paste. *Cem. Concr. Compos.* **2012**, *34*, 255–260. [CrossRef]
17. Tarannum, N.; Pooja, K.; Khan, R. Preparation and Applications of Hydrophobic Multicomponent Based Redispersible Polymer Powder: A Review. *Constr. Build. Mater.* **2020**, *247*, 118579. [CrossRef]
18. Yang, K.; Tang, Z.; Li, W.; Long, Z.; He, J.; Ma, G.; Li, Y.; Xiang, Y.; Xie, Y.; Long, G. A Comprehensive Review on the Toughening Technologies of Cement-Based Materials: From Multiscale Materials to Advanced Processes. *Constr. Build. Mater.* **2024**, *456*, 139274. [CrossRef]
19. Zhang, H.; Yao, S.; Wang, J.; Zhou, R.; Zhu, Y.; Zou, D. Tensile Properties of Sulfoaluminate Cement-Based Grouting Materials Toughened by in-Situ Polymerization of Acrylamide. *Constr. Build. Mater.* **2023**, *375*, 130885. [CrossRef]
20. Zhang, C.; Kong, X.; Lu, Z.; Jansen, D.; Pakusch, J.; Wang, S. Pore Structure of Hardened Cement Paste Containing Colloidal Polymers with Varied Glass Transition Temperature and Surface Charges. *Cem. Concr. Compos.* **2019**, *95*, 154–168. [CrossRef]
21. Wang, R.; Wang, P.; Peng, Y. Comparison of Three Characterization Methods for Flexibility of SBR Latex-Modified Cement Mortar. *J. Build. Mater.* **2010**, *13*, 390–394. [CrossRef]
22. Dong, F.; Mingkai, Z.; Deyong, J.; Qing, L. Investigation on the Relationship between Flexural Strength, Flexural Toughness and Impact Toughness of Styrene–Butadiene Rubber Latex-Modified Cement Concrete. *Mater. Res. Innov.* **2015**, *19*, S8-849–S8-854. [CrossRef]
23. Xu, F.; Zhou, M.K.; Shen, W.G.; Li, B.X. Study on the Toughness Performance of Polypropylene Fiber and SBR Polymer Latex Modified Cement Mortar. *AMR* **2009**, *79–82*, 1751–1754. [CrossRef]
24. Nataraja, M.C.; Dhang, N.; Gupta, A.P. Toughness Characterization of Steel Fiber-Reinforced Concrete by JSCE Approach. *Cem. Concr. Res.* **2000**, *30*, 593–597. [CrossRef]
25. Okamura, H.; Iwasaki, K.; Ozaka, Y.L.; Kakuta, Y. (Eds.) *Method of Test for Flexural Strength and Flexural Toughness of Steel Fiber Reinforced Concrete*; JSCE-SF4; Japan Society of Civil Engineering: Tokyo, Japan, 1984.
26. Kong, X.; Emmerling, S.; Pakusch, J.; Rueckel, M.; Nieberle, J. Retardation Effect of Styrene-Acrylate Copolymer Latexes on Cement Hydration. *Cem. Concr. Res.* **2015**, *75*, 23–41. [CrossRef]
27. Shah, S.P.; Carpinteri, A. (Eds.) *Fracture Mechanics Test Methods for Concrete*; RILEM TC89-FMT; Taylor & Francis: London, UK, 1991; ISBN 978-0-412-41100-7.
28. Jenq, Y.; Shah, S.P. Two Parameter Fracture Model for Concrete. *J. Eng. Mech.* **1985**, *111*, 1227–1241. [CrossRef]
29. Li, R.; Ton Loontjens, J.A.; Shan, Z. The Varying Mass Ratios of Soft and Hard Segments in Waterborne Polyurethane Films: Performances of Thermal Conductivity and Adhesive Properties. *Eur. Polym. J.* **2019**, *112*, 423–432. [CrossRef]
30. Suzuki, K.; Wakatuki, Y.; Shirasaki, S.; Fujita, K.; Kato, S.; Nomura, M. Effect of Mixing Ratio of Anionic and Nonionic Emulsifiers on the Kinetic Behavior of Methyl Methacrylate Emulsion Polymerization. *Polymer* **2005**, *46*, 5890–5895. [CrossRef]
31. Wang, M.; Wang, R.; Zheng, S.; Farhan, S.; Yao, H.; Jiang, H. Research on the Chemical Mechanism in the Polyacrylate Latex Modified Cement System. *Cem. Concr. Res.* **2015**, *76*, 62–69. [CrossRef]

Disclaimer/Publisher's Note: The statements, opinions and data contained in all publications are solely those of the individual author(s) and contributor(s) and not of MDPI and/or the editor(s). MDPI and/or the editor(s) disclaim responsibility for any injury to people or property resulting from any ideas, methods, instructions or products referred to in the content.